THE MARCONI REVIEW

Volume XXII Number 133 *Second Quarter* 1959

The Marconi Review is published four times a year
Annual subscription £1. Single copies 5s. Postage paid to any part of the world

EDITOR L. E. Q. WALKER A.R.C.S.

Marconi's Wireless Telegraph Company Limited, Baddow Research Laboratories
West Hanningfield Road, Great Baddow, Essex, England

Beam Aerials for Long Distance Telecommunications

In the mid 1920s significant changes were made in the technique of long distance point to point communication systems. Due to the new beam aerial designs, pioneered largely by C. S. Franklin, systems hitherto confined to long wave working were able to operate successfully in the HF spectrum (or so-called short waves) giving increased reliability and channel capacity. Any doubts about the improvements brought in by the new short wave beam systems were soon swamped in the flood of traffic that followed the change over, and communications in the HF band 10 Mc/s to 30 Mc/s has continued to be a very important and active feature of world wide systems to the present time.

The beam aerials which supplied the impetus for this departure in technique were designed to concentrate a high proportion of the available transmitter power into a beam aligned at a fairly low angle to the horizon in the direction of the co-operating station. Receiving aerials were likewise beamed and made capable of discriminating against unwanted signals. These aerials, operating at wavelengths between 3 metres and 100 metres, are in general either the standing wave type such as the dipole curtain arrays and the uniform current arrays, which radiate the beam in a direction approximately normal to the plane of the array (hence they are sometimes called broadside arrays), or the travelling wave type of aerial such as the rhombic or the H.A.D (Horizontal Array of Dipoles) which

radiate the beam approximately in the plane of the array. The rhombics, H.A.Ds and similar types are known as end-fire arrays. The aerials are supported on towers some 100 to 150 feet high and are constructed of wires carefully aligned in space. Considerable skill in rigging is required for their construction and maintenance. The feeder system to them is usually an open wire paired transmission line transformed to coaxial line and connected direct to the transmitter. These aerials are primary radiators. Their properties are derived from the phase relationships of the current flowing in the various parts of the wire structure. The standing wave aerials in particular usually have an associated reflector assembly to improve the directivity. These may take the form of a resonant curtain and switching can be provided to give beam reversal if required.

The angle of arrival of HF signals varies somewhat on a given circuit and this sets a limit to the narrowness of the beamwidth and consequently to the size of the aerial structure, the beamwidth being inversely proportional to the physical dimensions of the aerial aperture. Nevertheless HF directional aerials are large structures and wireless stations using them are characterized by their forests of towers and masts carrying vast cats cradles of wires.

In recent years considerable effort has been devoted to work on long distance communication systems making use of the scattering property of layers in the Ionosphere for Very High frequencies (30-60 Mc/s) and in the Troposphere for Ultra High frequencies (500-1,000 Mc/s). Although differences of opinion on the mechanism of scatter propagation exist among theoretical investigators, all are unanimous on the need for aerials having high directivity, to utilize fully the minute proportion of radio energy propagated in the required direction after scattering. For example, at the higher end of the frequency spectrum the path attenuation over a route of, say, 250 miles can amount to about 200 dB. Aerial efficiency and directivity are, therefore, very important. As in HF communication there is a limitation to the narrowness of the aerial beam but here for a different reason. For scatter propagation the aerials at each end of the link are aligned to illuminate a common volume of the scattering medium and the combined gains of the two aerials cannot be fully realized if this common volume is made too small. This effect has been designated "the aperture to medium coupling loss" and its value increases as the scattering angle increases and the aerials' beamwidths decrease. For most scatter link requirements, the coupling loss for aerials having beamwidths less than about 1° makes them a doubtful economic proposition.

Aerial designs for Ionospheric and Tropospheric scatter differ. The UHF aerials invariably follow the microwave or quasi-optical systems of a reflecting aperture illuminated by a primary source. In these systems the reflector is of double curvature forming either a spherical or paraboloid

surface. The paraboloid is by far the most common. The primary source is positioned at the focal point. It may be a horn (flared or straight), or a dipole with reflector, and it is connected by transmission line (waveguide or coaxial) to the transmitter. The relationship between the illumination of an aperture and its resulting re-radiation is well understood, and the primary source is dimensioned to produce a field distribution at the reflector aperture which will give rise to the required directional radiation diagram. The shape of this beam which is finally radiated is sometimes called the secondary radiation diagram.

The reflecting surface must fulfil a number of separate requirements. It must be formed to the paraboloid contours to a tolerance of about $\lambda/30$, in order to preserve the geometric property of the system. It must not permit more than a very small percentage of the R.F. energy incident on it to penetrate. An acceptable value for through transmission is 1% of the incident energy. It must fulfil these two conditions for simultaneously incident R.F. waves having mutually orthogonal polarization. This requirement follows from the wide practice of using a single aerial of this type for both transmitting and receiving (duplex operation) where decoupling between transmitter and receiver signals is provided by cross polarizing the signals. Experiments have confirmed that the transmitted polarization is preserved throughout this mode of propagation.

Mechanical requirements are important factors in the design of scatter reflectors. The rigidity of the structure should be adequate for it to maintain its contours within the specified tolerance under all the climatic conditions it is likely to meet. At the same time its rigidity and mass is limited by practical design considerations for the supporting structure. Wind loading on these reflectors influence the design of the reflector, its support structure, and the foundations in a fundamental manner. For example a typical reflector might be 60 feet in diameter with its centre raised 80 feet above ground level. In a 120 m.p.h. wind a solid surface reflector would cause an overturning thrust of about 80 tons to be imparted to the support structure. This figure could be reduced by 20% to 30% if the reflecting surface was open mesh construction of a size and shape to comply with the electrical requirements. An aerial structure subject to simultaneous wind and ice conditions would have to be designed as for a solid surface reflector. This applies, for example, to the "Dew Line" which is a chain of scatter stations on the North American Continent, situated about 400 miles north of the Arctic Circle.

Ionospheric scatter links using VHF aerials span distances of 500–1,400 miles. Scatter angles are steeper and beamwidth requirements are broader than for tropospheric scatter. Transmitter powers are high (about 40 kW) and the level of the side lobes and the backward radiation must be kept very low to safeguard against local interference and against multipath

back scatter which under bad conditions can reduce the transmission capacity of a link.

Aerials for this type of propagation do not belong properly in either the HF or the UHF categories. The wavelengths are too long to permit economic designs of the quasi-optical type and yet are short enough for aerials to be of a more compact type than the HF beam aerials. Arrays of stacked Yagis and corner reflector aerials are the two types most commonly in use.

The corner reflector is an interesting example of a transition from curtain array to paraboloid reflector. It has a linear array of dipole elements located near the apex of a V shaped sheet reflector. The beam is formed by the summation of the radiations from the dipole line and its images in the reflector. Solid reflecting surfaces would be quite impracticable at these wavelengths, and grids of wires parallel to the dipoles are used for the reflecting sheet. In view of the stringent minor lobe requirement the wire size and spacing must be judiciously chosen. Neither the corner reflector nor the Yagi array has the necessary symmetry to permit cross polarized duplexer operating and if duplexing is done, the separation between transmitter and receiver is achieved by means of filters.

Beam aerials are important and expensive items of equipment. When adding up the sum total of costs for radio equipment on a long distance link it will be found that the aerials and feeder system may account for between 30% and 60% of the total. It is proper therefore, that a commensurate amount of design effort be expended on them, particularly as no other product of radio engineering is so predominantly and constantly on public view.

A. KRAVIS

TRANSMISSION OF ELECTRO-MAGNETIC WAVES THROUGH WIRE GRATINGS (theory)

By J. K. SKWIRZYNSKI, B.Sc, A.R.C.S, and J. C. THACKRAY, B.Sc.

The authors consider the transmission properties of a plane polarized electromagnetic wave passed through a grating of cylindrical wires.

Only the case of normal incidence is treated, but a full theory is provided for a general angle of incidence. The transmission coefficient curves (amplitude and phase) cover wide ranges of the grating parameters and, by using normalization, frequency.

A possible application of the results to the design of waveguide filters, containing cylindrical inductive posts, is also given.

INTRODUCTION

The reflection properties of a surface composed of a grating of wires are of considerable interest in the design of microwave aerials. It is intended here to provide formulae for a general set of curves giving, in fact, the transmission loss of such a reflector for as wide as possible a range of wire diameters and spacings in terms of wavelength.

This particular diffraction problem was first studied by W. von Ignatowsky, who published several outstanding papers in the Annalen der Physik in 1912-14([1]). Interest in this work has revived again since 1939, but no essentially new contributions have appeared. The papers published ([2–6]) merely contain either publications of particular aspects of von Ignatowsky's theory or simplifications of that theory leading to straightforward formulae of a limited range of validity.

The transmission system is treated here in a general way, leading to explicit solutions of the boundary value problem. The numerical results have only been obtained for normal incidence of a vertically polarized electro-magnetic wave on the grating; however, the theory is presented for a general angle of incidence.

THE GEOMETRY AND MATHEMATICAL FORMULATION OF THE SYSTEM

Fig. 1 shows the intersection of a plane grating of circular metal cylinders with the (x, y) plane in cartesian space; the axes of the cylinders are perpendicular to this plane, a is the radius of the wires and b is the distance

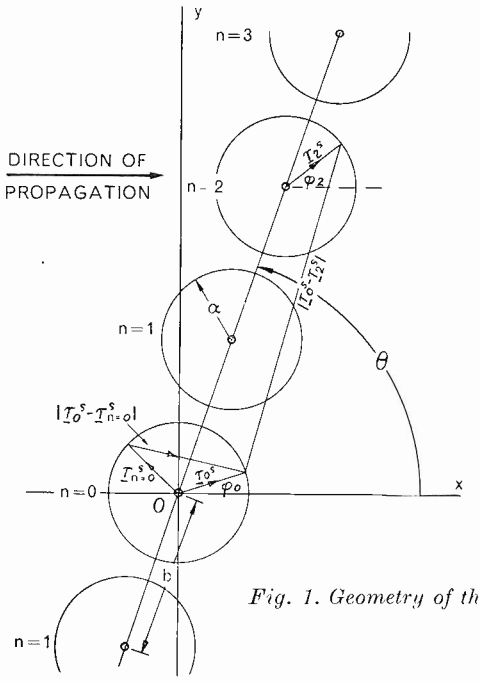

Fig. 1. Geometry of the plane grating

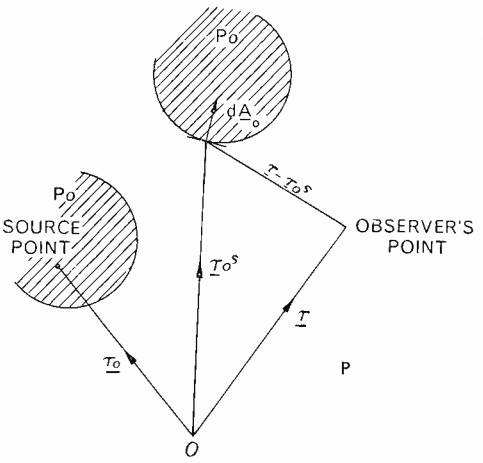

Fig. 2. Vectors used for Green's function

apart of their centres. The plane of the grating is inclined at an angle θ to the positive x-axis (for normal incidence $\theta = \frac{\pi}{2}$). The cylinders are numbered consecutively in the positive and negative directions, while the axis of the 0th cylinder coincides with the z-axis of the co-ordinate system. A plane electro-magnetic wave polarized in the z-direction is propagated in the positive x-direction and is scattered by the grating. The electric field component will contain the factor $\exp(jkx - j\omega t)$

$$\text{where } k = \frac{2\pi}{\lambda}$$

$$\omega = \frac{2\pi c}{\lambda}$$

c = velocity of light,

λ = wave length.

In the following analysis the implied time factor $\exp(-j\omega t)$ will be suppressed.

Let ψ be the electric field component. It will satisfy

$$\nabla^2\psi + k^2\psi = 0 \qquad (1)$$

and will vanish on the surface of each cylinder of the grating. The scattering problem can be solved with the help of the symmetrical Green's function $G(\underline{r} \mid \underline{r}_0)$, where $\underline{r}$ = position vector to the observer's point,

$\underline{r}_0$ = position vector to the source point.

Fig. 2 will serve to explain the nomenclature used in this formulation. Since the electric field vanishes on the cylinders,

$$\psi(\underline{r}^s_0) = 0 \tag{2}$$

where the superscript s denotes a position on the surface of a "source space" (in this case the surface of any cylinder acting as the source of scattered waves).

For these conditions, equation (1) can be integrated explicitly:

$$\frac{1}{4\pi}\oint_s G(\underline{r} \mid \underline{r}^s_0)\ [\mathrm{grad}_0\, \psi(\underline{r}^s_0)] \cdot d\underline{A}_0 = \begin{cases} \psi(\underline{r}) \text{ inside } P \\ 0 \text{ inside } P_0. \end{cases} \tag{3}$$

This solution gives ψ in terms of its boundary values and the Green's function. Since the system is essentially two dimensional (i.e. independent of the z-co-ordinate), the suitable Green's function is a Hankel function of the first kind:

$$G(\underline{r} \mid \underline{r}_0) = j\pi H_0^{(1)}(k \mid \underline{r} - \underline{r}_0 \mid), \tag{4}$$

which has a suitable logarithmic singularity as $\underline{r} \to r_0$ and satisfies the radiation conditions for an outgoing wave when $\mid r - \underline{r}_0 \mid \to \infty$.

The field component $\psi(\underline{r})$ in equation (3) is the sum of the incident field $\psi_{\mathrm{inc}}(\underline{r})$ and the scattered field $\psi_{\mathrm{sc}}(\underline{r})$, the latter being due to the induced currents on the surfaces of all cylinders. Hence, for the nth cylinder, let

$$\mathrm{grad}_0\, \psi(\underline{r}^s{}_{0n}) = \frac{1}{2\pi a} I_n(\phi_n), \tag{5}$$

where ϕ_n is the circumferential angle round the nth cylinder (see Fig. 1) and $\underline{r}^s_{0n}$ is the vector to a point on the surface of the nth cylinder (see Figs. 1 and 2). Hence (3) becomes

$$\psi(\underline{r}) = \psi_{\mathrm{inc}}(\underline{r}) + \frac{j}{8\pi}\sum_n \int_0^{2\pi} H_0^{(1)}(k \mid \underline{r} - \underline{r}^s_{0n} \mid) I_n(\phi_n)\, d\phi_n. \tag{6}$$

The scattered field in (6) is summed over all cylinders; these are identical and their number is infinite, so that each of them will be affected in the same way by all others, while the influence of the incident wave will be exhibited by a phase factor $\exp(jknb \cos\theta)$. The Fourier expansion of a circumferential current in (5),

$$I_n(\phi_n) = \exp(jknb \cos\theta) \sum_{s=-\infty}^{\infty} C_s \exp(js\phi_n) \tag{7}$$

can now be substituted in (6):

$$\psi(\underline{r}) = \psi_{\text{inc}}(\underline{r}) +$$

$$+ \frac{j}{8\pi} \sum_{\text{n}} \sum_{\text{s}} C_{\text{s}} \exp(jknb \cos\theta) \int_0^{2\pi} H_0^{(1)}(k\,|\,\underline{r} - \underline{r}^{\text{s}}_{0\text{n}}\,|\,) \exp(js\phi_{\text{n}})\, d\phi_{\text{n}}. \tag{8}$$

The field will be completely determined by (8) once the Fourier coefficients C_{s} are found.

DETERMINATION OF THE FOURIER COEFFICIENTS C_{s}

The total field vanishes on the surface of any cylinder. Since all cylinders are identical and are identically situated, the application of this boundary condition to any one of them will suffice. For convenience the 0th cylinder (see Fig. 1) will be chosen as the representative one. Thus, equating (8) to zero on the surface on the 0th cylinder, multiplying by $\exp(-jt\,\phi_0)$ and integrating over the whole range of ϕ_0, one obtains

$$T_{\text{t}} = -\sum_{\text{n}} \sum_{\text{s}} C_{\text{s}}\, R_{\text{snt}} \exp(jknb \cos\theta) \tag{9}$$

$$\left.\begin{aligned} \text{where } T_{\text{t}} &= \int_0^{2\pi} \psi_{\text{inc}}(\underline{r}^{\text{s}}_0) \exp(-jt\phi_0) d\phi_0, \\ R_{\text{snt}} &= \frac{j}{8\pi} \int_0^{2\pi} \int_0^{2\pi} H_0^{(1)}(k\,|\,\underline{r}^{\text{s}}_0 - \underline{r}^{\text{s}}_{\text{n}}\,|\,) \exp(j\,s\,\phi_{\text{n}} - j\,t\,\phi_0)\, d\phi_{\text{n}}\, d\phi_0. \end{aligned}\right\} \tag{10}$$

Since $\psi_{\text{inc}}(\underline{r}^{\text{s}}_0) = \exp jkx = \exp(jka\cos\phi_0)$

$$= \sum_{q=-\infty}^{\infty} j^q J_q(kA) \exp(jq\,\phi_0),$$

then $T_{\text{t}} = 2\pi j^{\text{t}} J_{\text{t}}(ka)$. (11)

The evaluation of R_{snt} is tedious but quite straightforward (by using the Fourier expansion of Hankel functions([7])).

For $n = 0$,

$$R_{\text{s0t}} = \frac{1}{2} j\pi J_{\text{t}}(ka)\, H_{\text{t}}^{(1)}(ka)\, \delta_{\text{st}} \tag{12}$$

(where $\delta_{\text{st}} = 0$ when $s \neq t$, $\delta_{\text{st}} = 1$ when $s = t$).

For $n > 0$,

$$R_{\text{snt}} = \frac{1}{2} j\pi J_{\text{s}}(ka)\, J_{\text{t}}(ka)\, H_{\text{t}-\text{s}}^{(1)}(knb) \exp[j(s-t)\,0]. \tag{13}$$

For $n < 0$, θ in (13) is replaced by $(\theta + \pi)$.

Substituting (11) — (13) into (9) and dividing by $-\frac{1}{2} j\pi J_t(ka)$, one obtains

$$4j^{t+1} = H_t^{(1)}(ka)\, C_t + \sum_s C_s J_s(ka) \exp[j(s-t)\theta] \sum_{n=1}^{\infty} H_{t-s}^{(1)}(knb) [\exp(jknb\cos\theta) + (-1)^{s-t} \exp(-jknb\cos\theta)]. \quad (14)$$

This infinite set of equations has to be solved simultaneously for C_s.

EVALUATION OF THE TRANSMISSION COEFFICIENT FOR NORMAL INCIDENCE

For normal incidence $\left(\theta = \frac{\pi}{2}\right)$, equations (14) become

$$4j^{t+1} = C_t H_t^{(1)}(ka) + 2 \sum_s C_s J_s(ka) \cos\left[\frac{\pi}{2}(s-t)\right] \sum_{n=1}^{\infty} H_{t-s}^{(1)}(knb). \quad (15)$$

The sum of Hankel functions (over n) has been evaluated by von Ignatowsky (op. cit., p. 425, equ. 21). For the time being, let

$$\sum_{n=1}^{\infty} H_{t-s}^{(1)}(knb) = \frac{2j}{\pi} G_{t-s}(kb). \quad (16)$$

The function $I_n(\phi_n)$ defined in (5) and (7) represents the effective circumferential current of the nth cylinder. For normal incidence this current distribution is an even function of the angle ϕ_n, so that

$$C_s = C_{-s}. \quad (17)$$

Substituting (16) and (17) in (15),

$$4j^{t+1} = \frac{4j}{\pi} C_0 J_0(ka)\, G_t(kb) \cos\frac{\pi t}{2} + C_t H_t^{(1)}(ka) + \frac{4j}{\pi} \sum_{s=1}^{\infty} C_s J_s(ka) \left\{ G_{t-s}(kb) \cos\left[\frac{\pi}{2}(t-s)\right] + (-1)^s G_{t+s}(kb) \cos\left[\frac{\pi}{2}(t+s)\right] \right\}. \quad (18)$$

Writing

$$\left.\begin{aligned} C_0 &= -\frac{2\pi V_0}{J_0(ka)}, \\ C_s &= (-1)^{s+1}\frac{\pi V_s}{J_s(ka)} \quad (s \neq 0) \end{aligned}\right\} \tag{19}$$

and

$$\left.\begin{aligned} W_0 &= \frac{1}{2} j\pi \frac{H_0^{(1)}(ka)}{J_0(ka)}, \\ W_s &= \frac{1}{4} j^{s+1}\pi \frac{H_s^{(1)}(ka)}{J_s(ka)} \quad (s \neq 0), \end{aligned}\right\} \tag{20}$$

equations (18) can be written in a more convenient form:

$$\left.\begin{aligned} (V_0 W_0 - 1) &= 2\sum_{s=0}^{\infty}{}' (-1)^s V_{2s} G_{2s}, \\ (V_{2t} W_{2t} - 1) &= \sum_{s=0}^{\infty}{}' (-1)^s V_{2s}\left[G_{2t-2s} + G_{2t+2s}\right], \\ j(V_{2t-1} W_{2t-1} - 1) &= \sum_{s=1}^{\infty}{}' (-1)^s V_{2s-1}\left[G_{2t-2s} + G_{2t+2s-2}\right]. \end{aligned}\right\} \tag{21}$$

The coefficients V_s (which in turn determine C_s) are given here in terms of the cylindrical functions $W_s(ka)$ depending on the cylinder radius a and of the functions $G_s(kb)$ depending on the cylinder separation b. The latter functions are in fact the complex conjugates of the S function employed by von Ignatowsky, and V_s corresponds to his D_s, except for a constant phase difference of π due to the nature of the time dependence.

In his 1914 paper, von Ignatowsky breaks down the summation of the Hankel functions into four simpler sums, and, keeping b less than a quarter wave-length, the expressions he uses can be conveniently truncated to

and

$$\left.\begin{aligned} G_0 &\doteq \frac{1}{2}\ln\left(\frac{2\lambda}{\gamma b}\right) - j\left(\frac{\lambda - \pi b}{4b}\right) \\ G_{2s} &\doteq \frac{1}{4s} - \frac{(2\lambda)^{2s} B_s}{8s\, b^{2s}} - \frac{j\lambda}{4b} \end{aligned}\right\} \tag{22}$$

where γ is Euler's constant ($\ln \gamma = 0{\cdot}5772\ldots$) and B_s is a Bernoulli number. A more accessible reference is equation (18) of Infeld, Smith and Chien[8].

NUMERICAL RESULTS

The initial local interest in this subject([9]) was confined to the amplitude of the transmitted field, with possible extension to consider oblique incidence. To some extent, this explains the range of possibilities computed. Expressing wire radius and separation as multiples of wavelength, the smallest likely radius was 0·0025%, the minimum separation was twice the wire diameter and the radius was to be increased until, at this minimum spacing, 60 decibels transmission loss was reached, while the maximum separation was to be such that there was 3 decibels transmission loss. The computation required to produce a useful set of curves presents a rather formidable appearance, and some consideration of it may therefore be useful.

The infinite set of simultaneous equations in (21) can be replaced by one or more of such equations, and so orders of approximations will exist corresponding to the number taken, and hence to the number of coefficients, V_s, found.

The evaluation of V_s is tedious and, since W_s is a function of the wire radius and G_s is a function of the separation, it is best expressed in algebraic terms for each order of approximation and then computed. Thus, the first approximation, taking into account only V_0, gives, substituting for W_0 and G_0,

$$V_0 = \frac{-1}{2\left[\frac{Y_0(ka)}{J_0(ka)} + \frac{2}{\pi}\ln\left(\frac{2\lambda}{\gamma b}\right) - j\frac{\lambda}{\pi b}\right]} \tag{23}$$

Similarly, the second approximation, taking into account only V_0 and V_1, gives V_0 as in (23) and

$$V_1 = \frac{j}{\frac{Y_1(ka)}{J_1(ka)} + \frac{2}{\pi}\ln\left(\frac{2\lambda}{\gamma b}\right) + \frac{1}{\pi} - \frac{2\lambda^2 B_1}{\pi b^2} - j\frac{2\lambda}{\pi b}} \tag{24}$$

Further approximations become much more complicated to write out, and in practice G_s and W_s are better computed separately. Thus, if one writes

$$G_0 = x_0 + j\left(y + \frac{\pi}{4}\right),\ G_{2s} = x_{2s} + jy,$$

$$W_0 = \frac{j\pi}{2}[1 + jR_0(ka)],\ W_s = j^{s+1}\frac{\pi}{4}[1 + jR_s(ka)], \tag{25}$$

solutions (23) and (24) become

$$V_0 = \frac{-\pi}{2(\pi R_0 + 4x_0 - j4y)} \text{ and } V_1 = \frac{j\pi}{\pi R_1 + 4(x_0 + x_2 - 2y)} \tag{26}$$

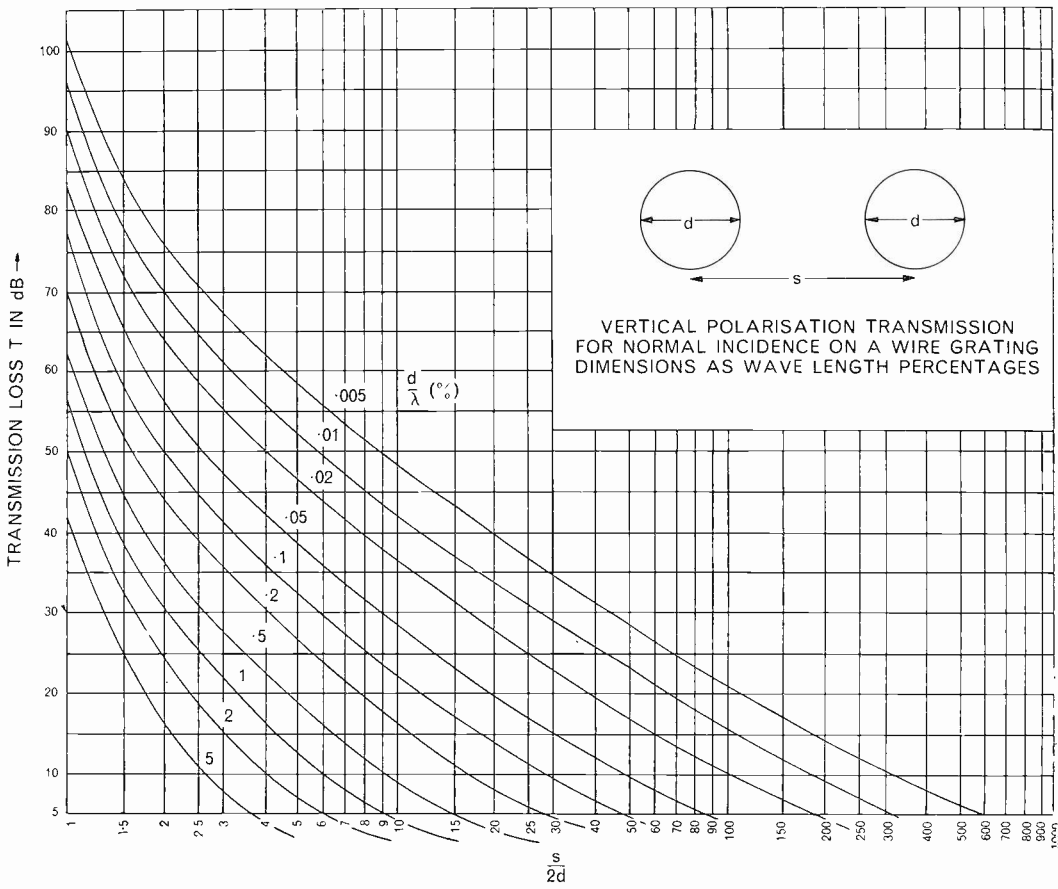

Fig. 3. Transmission loss coefficient

respectively, which is much more convenient. This is important, since much of the computation is concerned with producing transmission ratios of the order of — 40 decibels or less, and a high degree of accuracy is needed in the working.

Once V_s is known, the amplitude and phase of the transmitted field can be found. If equation (8) is summed in the same way as it was to produce the simultaneous equations for C_s in (18), and then normalized by the incident field, one obtains

$$\frac{\psi_{\text{total}}(\underline{r})}{\psi_{\text{inc}}(\underline{r})} = 1 + \frac{\lambda}{2b}\sum_{s=0}^{\infty}(-1)^s j^{s+1} V_s^* \equiv T \exp(j\Phi), \qquad (27)$$

which is the transmission ratio.

The first and second approximations were first computed jointly, to decide whether the second approximation was good enough, in so far as it showed no appreciable difference from the first. In cases where the

separation was too small for this, the fourth approximation was used instead, since it was noticed that the even order approximations gave the greater improvement. It was decided to go no further than this approximation, because the results from a pilot computation for a 2·5% wire radius gave the transmission sufficiently convergently (comparing each approximation to the next up to the sixth), to make appropriate slight corrections possible to all results within the range of computation. It seems very unlikely that at the minimum separation there would be more than one or two units of inaccuracy in the fourth decimal place of the decibel equivalents.

The curves shown in Figs. 3 and 4 have their parameters expressed by symbols, s and d, more usual for engineering practice. They show the theoretical transmission loss coefficient, T and its phase Φ, over a very wide range of wire radius and separation, in terms of wave-length, and are

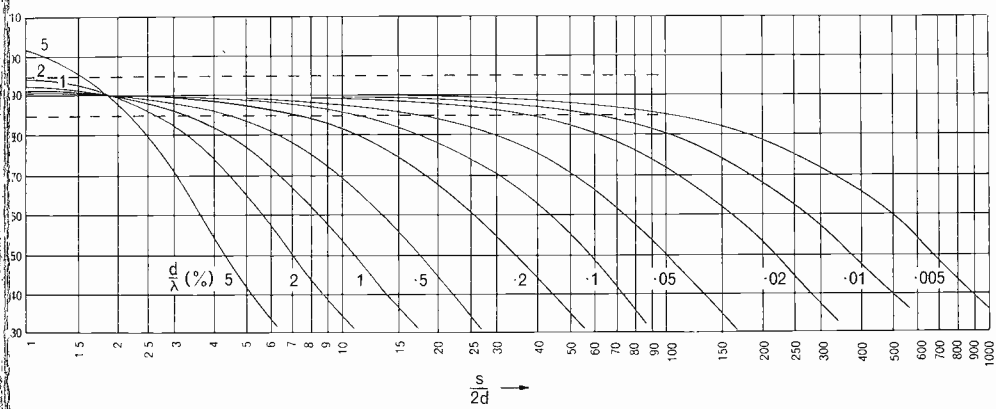

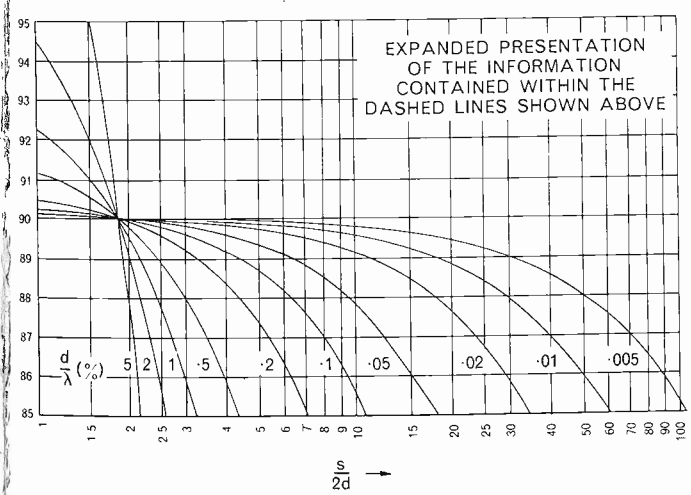

Fig. 4. Phase of transmission coefficient

valid for most frequencies reasonably to be expected. The apparently common point of 90° phase for all wire radii is at the value $\frac{s}{2d} \fallingdotseq 1{\cdot}86$.

These curves will give a convenient value as a guide to the transmission amplitude for oblique incidence if the approximating factor sin θ is used to modify the normal incidence value. The quantities s and d are expressed in terms of wavelength, and the user must realize that if d is a percentage then s is also a percentage.

POSSIBLE APPLICATIONS TO THE DESIGN OF WAVEGUIDE FILTERS

The simplest obstacle used in waveguide transmission to obtain an impedance element consists of one or more thin cylindrical inductive posts placed across the narrower dimension of the guide. Consider a series of n equidistant posts as shown in Fig. 5 (where $n = 3$).

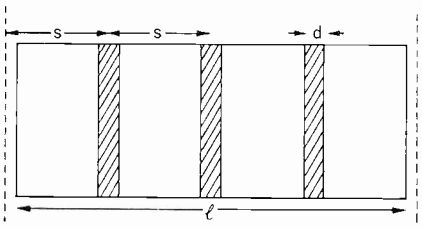

Fig. 5. Three equidistant posts in a waveguide

In order to ensure exact identification of the parameters of the wire grating previously considered with the waveguide and obstacle dimensions, let the width of a guide be

$$l = (n + 1)\, b - 2a \tag{28}$$

where b and a are defined both in Fig. 1 and Fig. 5. The transverse electric field vector (H_{10} mode) in the plane of the posts shown in Fig. 5 satisfies the same boundary conditions as the scalar function ψ considered above. Hence, the transmission properties of the present wire grating can be used with reasonable accuracy to derive the equivalent transmission coefficient and thence the equivalent shunt reactance of a series of equidistant cylindrical inductive posts in a waveguide. The approximation involved here is due to the fact that, whereas the transverse electric field vanishes on the vertical walls of the waveguide shown in Fig. 5, in the present model it only vanishes on the surface of the two wires representing these vertical walls.

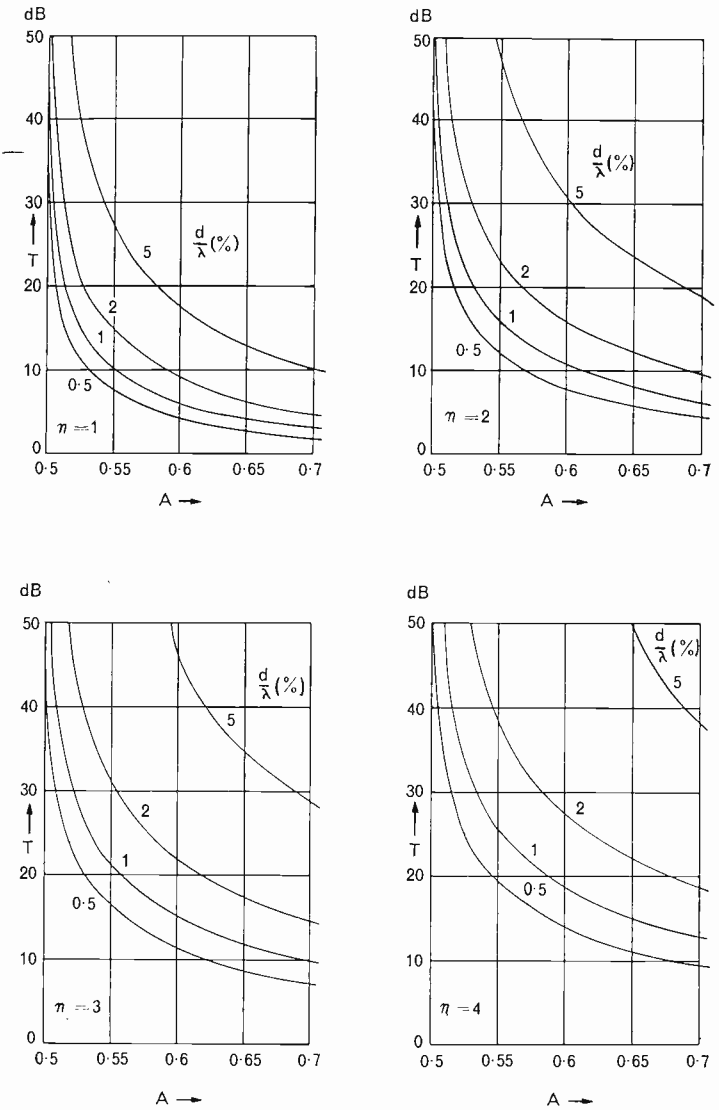

Fig. 6. Transmission loss coefficient for n posts in a waveguide

Let λ and λ_g be the free space and guide wavelengths, respectively. Then for the H_{10} mode

$$\frac{1}{\lambda_g} = \frac{1}{\lambda}\sqrt{1 - \left(\frac{\lambda}{2l}\right)^2} \tag{29}$$

Hence, if

$$A = \frac{l}{\lambda} = \frac{lf}{c} \tag{30}$$

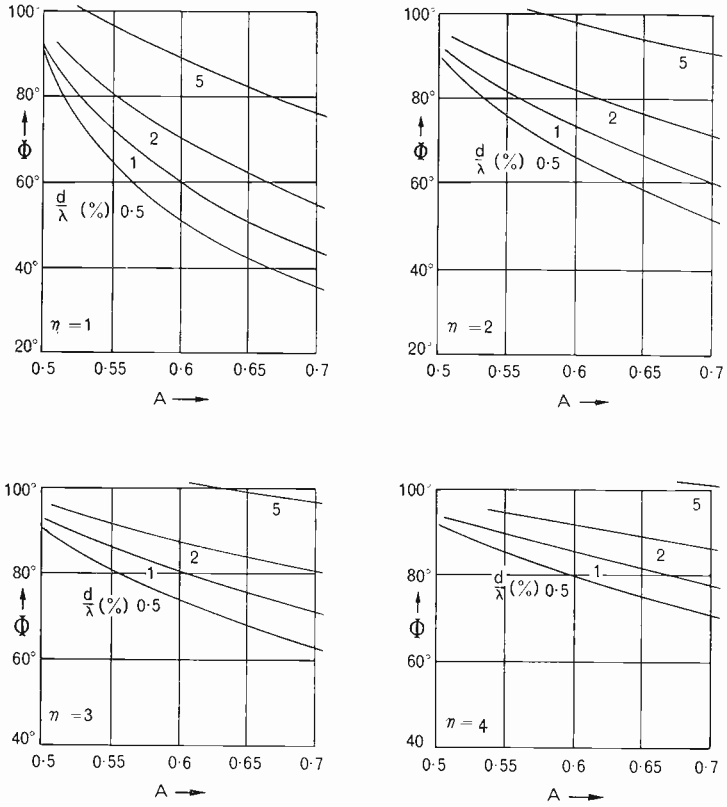

Fig. 7. Phase of transmission coefficient for n posts in a waveguide

is the frequency factor (f is the frequency while c is the velocity of light in free space) then

$$\frac{\lambda_g}{\lambda} = \frac{2A}{\sqrt{4A^2 - 1}} \quad \text{and} \quad \frac{l}{\lambda_g} = \frac{1}{2}\sqrt{4A^2 - 1}\,. \tag{31}$$

Also, since from (28)

$$l = \lambda_g\,[(n + 1)\,s - d], \tag{32}$$

the parameter used to plot the transmission coefficient in Figs. 3 and 4 becomes

$$\frac{s}{2d} = \frac{2d + \sqrt{4A^2 - 1}}{4(n + 1)d}\,. \tag{33}$$

Hence, given the frequency factor A, defined in (30), the number of posts n and the post diameter $d = \dfrac{2a}{\lambda_g}$ as a fraction of guide wavelength, one can

read off the amplitude and phase of the relevant transmission coefficients in Figs. 3 and 4.

The useful range of the frequency factor, $\frac{1}{2} < A < \frac{1}{\sqrt{2}}$, was used to obtain Figs. 6 and 7, where the amplitude T and the phase Φ are given for four values of d, namely 5%, 2%, 1% and 0·5%, of the guide wavelength, for $n = 1$, 2, 3 and 4 posts spaced at equal distances across the guide.

Given the transmission coefficient $T \exp(j\Phi)$, the corresponding reflection coefficient becomes[10], for

$$0 < \Phi < 90°,$$

$$R = \sqrt{1 - T^2} \exp\left[j\left(\Phi - \frac{\pi}{2}\right)\right]. \tag{34}$$

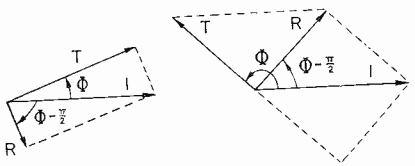

Fig. 8. Reflection and transmission coefficients

This relation between the reflection and transmission coefficients becomes evident from Fig. 8. Finally, the reflection coefficient of a reactance jX placed across the guide is[11]

$$R = -\frac{1}{1 + 2jX}, \tag{35}$$

so that

$$2jX = -\sqrt{1 + 2m\sin\Phi + m^2} \exp\left[j \tan^{-1}\left(\frac{m\cos\Phi}{1 + m\sin\Phi}\right)\right] \tag{36}$$

where

$$m = \frac{1}{\sqrt{1 - T^2}} = |R|^{-1}. \tag{37}$$

Since generally, $T^2 < 0{\cdot}1$ and Φ does not deviate appreciably from $\frac{\pi}{2}$ in the range shown in Figs. 6 and 7, it is simpler to consider these quantities expressed as

$$T^2 = 4\delta \text{ and } \Phi = \frac{\pi}{2} - \varepsilon$$

where δ and ε are small. Then (36) yields the approximation

$$jX = (1 + \delta) \exp\left[j\left\{\pi + \frac{\varepsilon}{2}(1 + \delta)\right\}\right] \qquad (38$$

which isolates the divergence of X from its boundary value of j conveni ently over most of the range in question.

REFERENCES

1 W. von Ignatowsky: *Ann. der Phys.* 44, p. 369 (1914).
2 W. Wessel: *Hochfrequenztechnik* 54, p. 62 (1939).
3 G. G. MacFarlane: *J.I.E.E.* 93, 10 (IIIA), p. 7 (1946).
4 G. von Trentini: *Z. angew. Phys.* 5, p. 221 (1953).
5 J. R. Wait: *Can. J. Phys.* 32, p. 571 (1954).
6 J. R. Wait: *Appl. Sci. Res.* B4 p. 393 (1954).
7 G. N. Watson: *Theory of Bessel Functions.* 2nd ed. Cambridge University Press.
8 L. Infeld, V. G. Smith and W. Z. Chien: *Jour. Math. Phys.* XXVI, p. 22 (1947).
9 E. G. A. Goodall and J. A. C. Jackson: see following article.
10 R. A. Waldron and J. K. Skwirzynski: *Note on Reflection Coefficients* (to be published)
11 L. Lewin: *Advanced Theory of Waveguides.* Iliffe and Sons, London (1951).

RADIO INDUSTRY COUNCIL PREMIUMS

Each year, the Radio Industry Council awards six premiums, each of 25 guineas, for articles on Radio and Electronics published in the technical press.

A premium was awarded this year for the article entitled "A New High-Efficiency Amplifier" by V. J. Tyler, B.Sc, A.M.I.E.E, which appeared in the *Marconi Review*, 3rd Quarter 1958, No. 130.

Speaking at a luncheon of the Radio Industry Council at which the awards were presented, Mr. L. T. Hinton, Chairman of the Electronic Engineering Association, said

"These articles are not only helpful to British industry, but the prestige and standing of British research and engineering in the countries of the world can be greatly enhanced by the standard of technical writing The product we sell is highly technical, we sell it to technical customers and good authoritative, well presented and well distributed technical writing does more to help our vital exports than all the glossy brochures put together."

TRANSMISSION OF ELECTRO-MAGNETIC WAVES THROUGH WIRE GRATINGS (experimental)

by E. G. A. GOODALL, M.Sc. and J. A. C. JACKSON, Assoc.Brit.I.R.E.

An experimental investigation into the transmission of vertically polarized electro-magnetic waves through a plane vertical grating of circular cross section wires has been made. A comparison is made between experimental and theoretical values of power transmitted at normal incidence for gratings with wire diameters such that $d\% = 2$ & 5 $\left(d\% = 100\,\frac{d}{\lambda}\right)$. *A measurement has also been made of the power transmitted through a wire grating for* $d\% = 2$, *for angles of incidence between* $5°$ *and* $50°$.

INTRODUCTION

If normally incident linearly polarized electro-magnetic radiation falls on an infinite grating of circular wires then when the electro-magnetic vector is perpendicular to the wires most of the energy is transmitted. When the electric vector is parallel to the wires a large proportion of the incident energy is reflected. This principle results in two applications in the field of microwave antenna design.

A solid reflecting surface of a microwave reflector may in certain cases be satisfactorily replaced by a parallel rodded structure set on a given profile. A comparison of such an arrangement with that of a solid reflector may be listed as follows:

(a) Reduction in weight which leads to a saving in cost in the turning gear.
(b) Effect of windage is slightly reduced but not to the extent that at first might be expected(1).
(c) Ease of construction—but the actual reflecting surface is difficult to define.
(d) A rodded structure is polarization sensitive which may or may not be an advantage in certain applications.

The second application of a wire grating structure in microwave antenna work is in the elimination of cross polarized sidelobes which occur on a shunt inclined slotted linear array. This simply consists of placing a grid of vertical wires in front of the array which transmits horizontal polarization in order that the vertically polarized component be reduced.

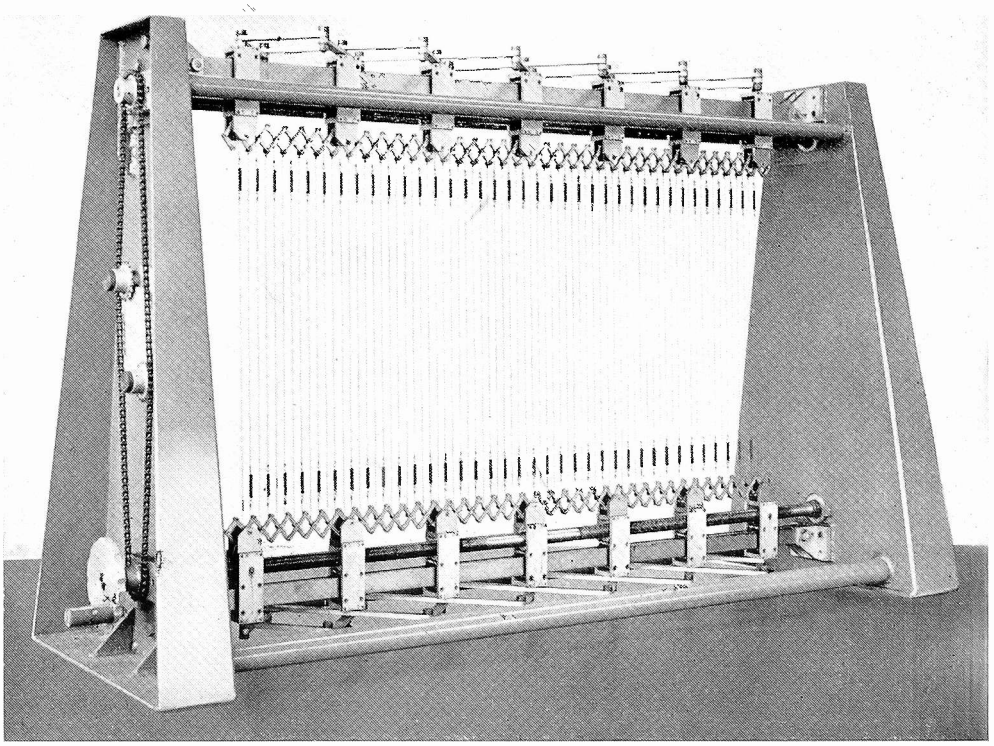

Fig. 1. Variable grating

The exact proportion of energy transmitted through a grid of given spacing and wire diameter must be known before being applied in the above two applications. An empirical expression exists which gives for certain wire spacings a value for the amount of energy leaking through a grid when the incident polarization is parallel to the wires(2).

If T^2 = percentage power transmitted
S = centre to centre spacing between wires
d = diameter of each wire

then $$T = 4{\cdot}6 \frac{S}{\lambda} \log_{10} \frac{S}{\pi d} \quad \ldots\ldots\ldots (1).$$

Examination of the above expression shows that when $\frac{S}{d}$ approaches π, the percentage power leaking through the grating becomes zero. In practice this does not occur, T^2 only approaching this value as S approaches d i.e., as the wires touch one another.

A theoretical investigation has been made in order to obtain a general expression for power transmitted through a grating of circular wires. The

results for values of $\frac{S}{2d}$ of 1 to 1,000 and $d\%$ of 5 to 0·005 are shown graphically([3]). In order to test the validity of the mathematical expression derived in the above work especially for the region where $\frac{S}{d}$ approaches π, some accurate checks have been made.

DESCRIPTION OF APPARATUS

The requirement that the wires of circular cross section be arranged in a vertical plane and parallel to one another was achieved by using a set of "lazy tongs" attached to both the top and the bottom of the vertical wires. With this system movement at one end enabled all the wires to be moved by the same amount, thus parallel uniformity was maintained, whilst the distance between centres of wires could be increased or decreased (Fig. 1). In the grating used, S the spacing of the wires was variable from $\frac{1}{2}$ inch to $\frac{1}{8}$ inch and the overall size of the grating was 36 inches $\times$ 13½ inches when fully extended.

The performance of the grating was then measured using X band frequencies since suitable test apparatus was available and, using wires of a practical diameter, $\frac{d}{\lambda}$ values frequently used in aerial design could be conveniently checked. In order to decrease reflections from neighbouring objects and to ensure that all the radiation transmitted passed through the finite grating a lens system was used (Fig. 2). Plane polarized electromagnetic radiation from a horn of aperture 18·9 cms $\times$ 14·9 cms illuminated the 2 foot diameter perspex lens. The grating was then placed at the conjugate focal point of this lens and, on the far side of the grating from the lens, a receiving horn identical to the one described above was placed.

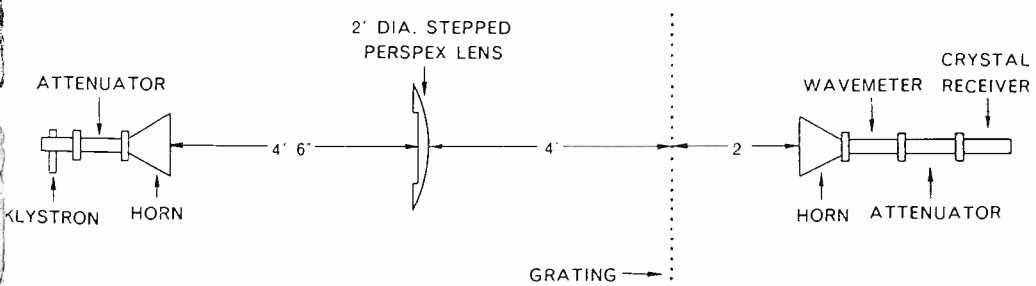

Fig. 2. Schematic diagram of apparatus

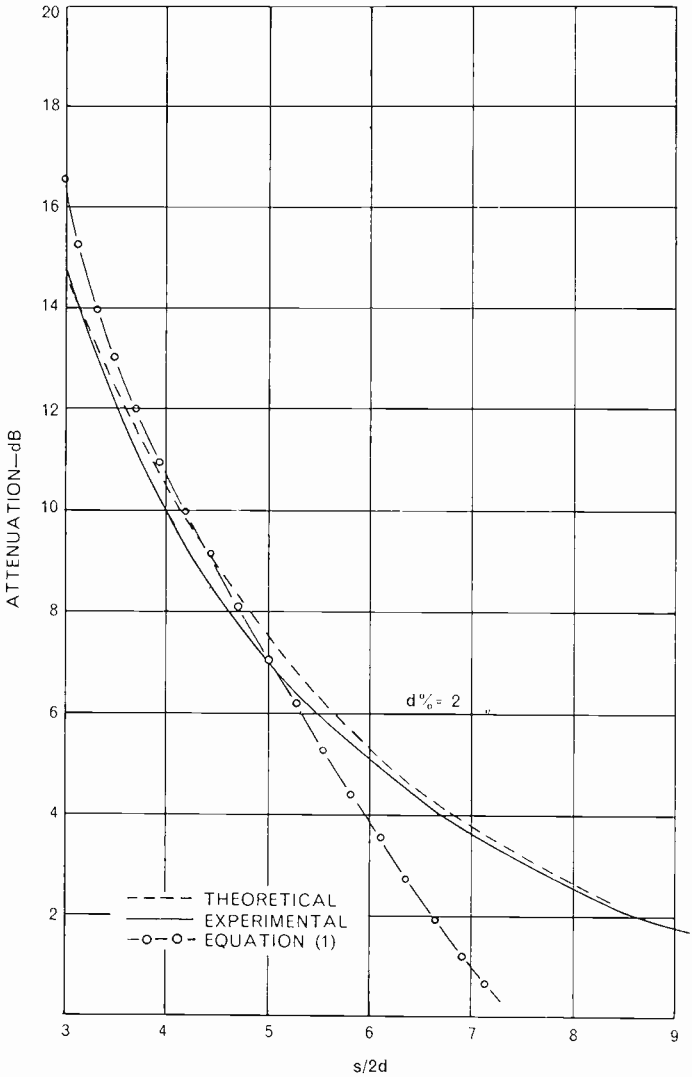

Fig. 3. Transmission through a plane grating $\lambda = 3{\cdot}55$ *cm.*

NORMAL INCIDENCE MEASUREMENTS

In practical aerial design the $d\%$ value is usually taken to be in the region of 5 to 15% with $\frac{S}{2d}$ lying between 1·25 and 1·7. If equation (1) is used to determine a transmission loss for gratings having these values, no reliable conclusions may be drawn since the equation is invalid in this region.

Using the apparatus previously described, the percentage power passing through the grating was determined for a particular wire diameter and for various wire spacings. These values were then compared to the amount of radiation received when the grating was absent; thus a relative

value of the transmitted energy through the grating could be determined. Standing waves present in the system were minimized with padding attenuators, and an average value of the remaining standing waves was then recorded for each individual measurement. In all measurements the receiver was calibrated against a standard rotary vane attenuator.

The transmission properties of a grating with wires of 0·028 inches diameter checked at X band enabled the $d\% = 2$ curve to be compared to the theoretical curve of Thackray and Skwirzynski[3] over a $\frac{S}{2d}$ range of three to nine (Fig. 3). Changing the grating wires to 0·068 inches diameter enabled a similar comparison to be made for the $d\% = 5$ curve for

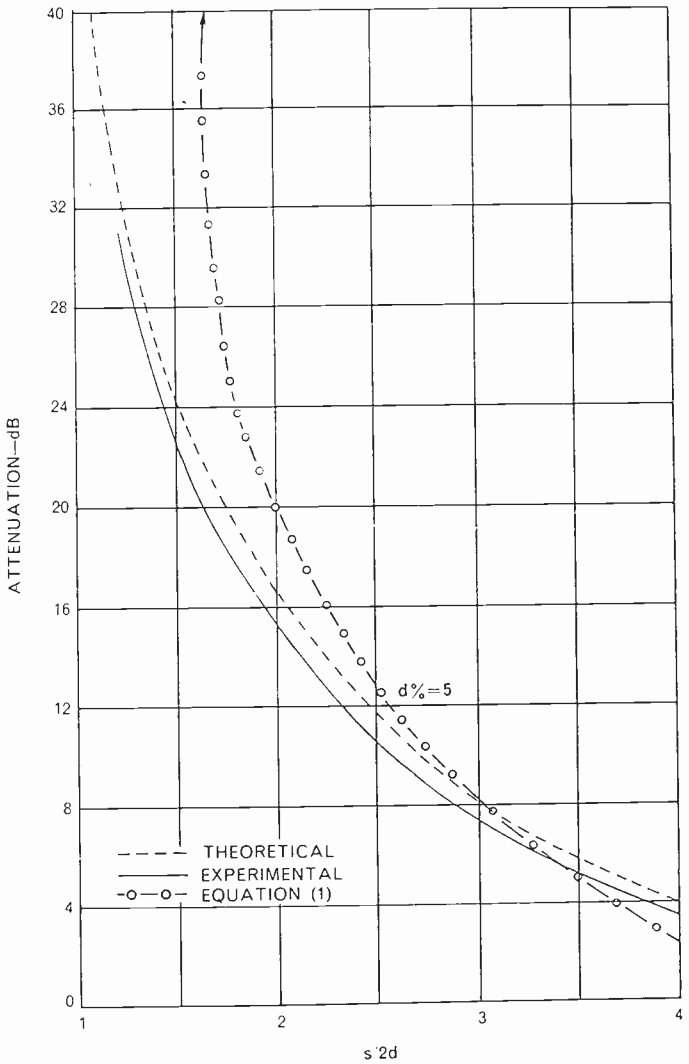

Fig. 4. Transmission through a plane grating $\lambda = 3{\cdot}3$ *cm.*

a $\frac{S}{2d}$ range of one to four (Fig. 4).

For the electric vector perpendicular to the wires for $\frac{S}{2d} = 1{\cdot}285$ and $d\% = 5$ the measured transmitted loss was 0·15 dB, whilst the transmission through the grating with the electric vector parallel to the wires was — 29 dB.

TRANSMISSION FOR OBLIQUE ANGLES OF INCIDENCE

When the wire spacing S is less than $\frac{\lambda}{2}$ of the radiation being used, and the wire radius $\frac{d}{2}$ is much less than S, a plane wave with its electric vector parallel to the wires incident at an angle $+ \alpha$ from the normal gives rise to a reflected wave at angle $- \alpha$ and a transmitted wave in the original direction. Surface waves do not occur unless $\frac{2\lambda}{d} < \left(1 + \sin \alpha\right)$ [4].

In the experimental arrangement for measurement of transmission loss with oblique angles of incidence the grating was placed on a turntable so that angles of incidence from 5° to 50° could be covered. With this arrangement measurements similar to the normal incidence case were again made over a range of values of $\frac{S}{2d}$ (determined by a given wire diameter) and for incident angles from 5° to 50°. A grating with a given diameter of wire and with the range of frequencies available predetermined the $d\%$ values that could be checked. Thus with wires of 0·028 inches diameter and a wavelength of 3·55 cms the $d\% = 2$ curve was obtained (Fig. 5).

CONCLUSIONS

Excellent agreement was found between experimental and theoretical curves for $d\% = 2$ (Fig. 3). In the region where $\frac{S}{2d}$ approaches $\frac{\pi}{2}$ there appeared to be a slight deviation between the two curves. This deviation may be due to the now small width of the grating which has decreased to approximately one quarter its original width. For the $d\% = 5$ curves the deviation between the theoretical and experimental curves is a constant quantity (Fig. 4). With the $d\% = 5$ curve, $\frac{S}{2d}$ has been varied from 1·28 to 3·94 and has passed through the value of $\frac{\pi}{2}$. No discontinuity appeared and the agreement between theoretical and experimental curves was good.

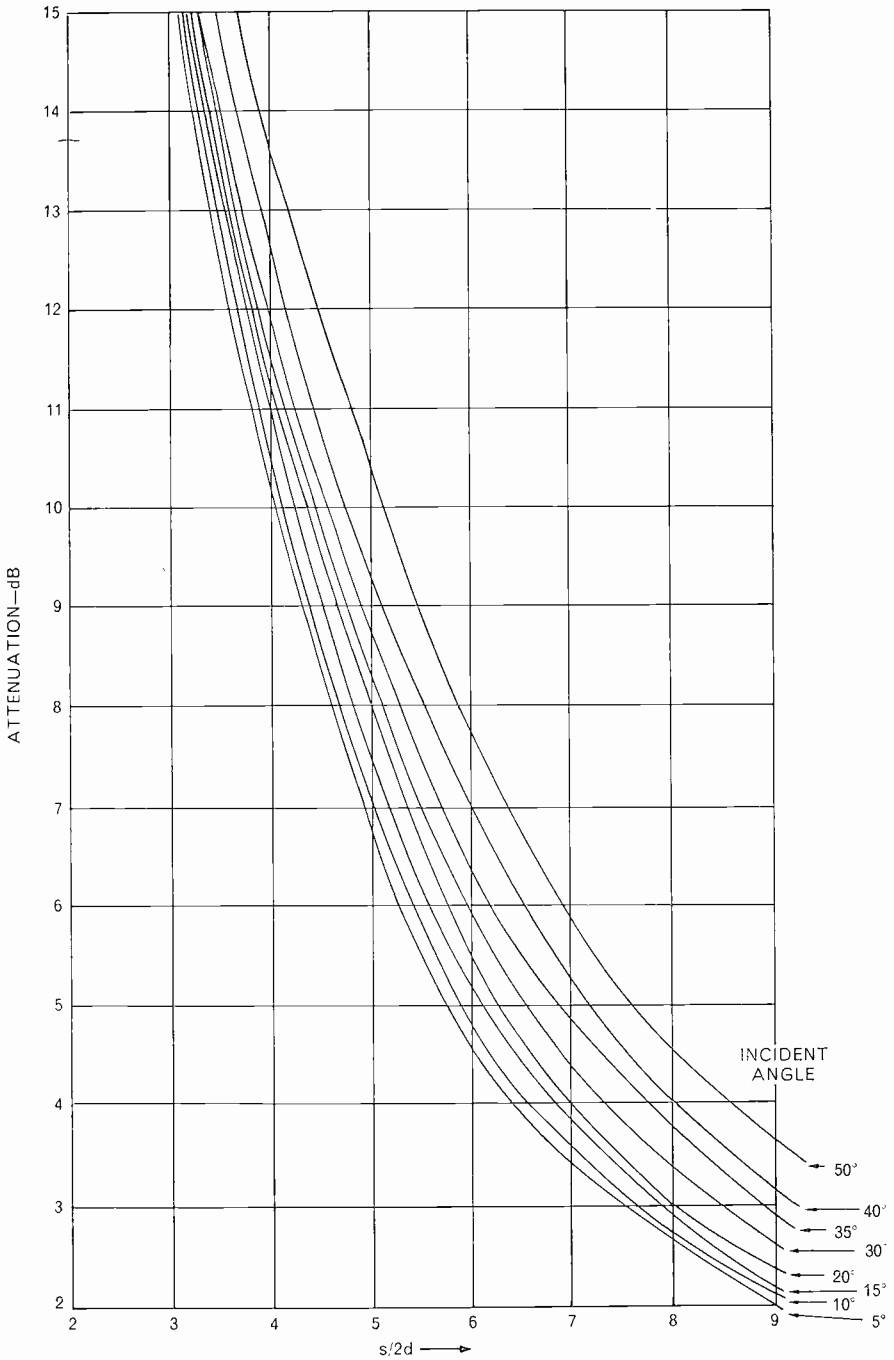

Fig. 5. Transmission through a plane grating for various angles of incidence d% = 2

ACKNOWLEDGMENTS

The work described in this paper was incidental to an Admiralty Contract.

REFERENCES

1 Radar Scanners and Radomes. *MIT Rad. Lab. Series No.* 26, p. 33-38 (1948).
2 R. A. SMITH: *Aerials for Metre and Decimetre Wavelengths*, p. 79 (Cam. Univ. Press) (1949).
3 J. SKWIRZYNSKI and J. THACKRAY: *Marconi Review*, this issue, p. 77
4 G. G. MACFARLANE: Surface Impedance of an Infinite Parallel Wire Grid at Oblique Angles of Incidence. *J.I.E.E.*, Vol. 93, Pt. IIIA, p. 1523 (1946).

BOOK REVIEW

RADIO ENGINEERING FORMULAE AND CALCULATIONS *by W. E. Pannett*

George Newnes Ltd, London. Price 17s. 6d.

Radio engineers and students have a wide variety of text books from which to select their reading, many of these volumes providing adequate mathematical formulae and analyses for most of their tasks. It is a great convenience nevertheless to have in one handy volume many of the formulae that occur from time to time in one's study or work. Students and some engineers will therefore welcome the book under review by an author who is well known to Marconi employees as their one-time Chief of Installations Drawing Office. Many of them will already know of the contents, most of which has appeared in the *Radio and Television Engineer's Reference Book*, as Section I "Formulae and Calculations", the present material being a reprint from this with some additions.

The text, which is well illustrated, has been divided into four sections dealing respectively with aids to engineering students; formulae and examples; units and symbols; and mathematical formulae, data and tables. More than three quarters of the text relates to formulae and examples, and covers the whole gamut of radio subjects from Ohm's law and circuit theorems to water and air cooling of high power valves, modulation, television transmitters, radar transmitters, aerials and propagation, and great circle bearings. Receivers are not neglected and formulae and examples are given in respect of receiver problems and characteristics, amplifiers, resonant and coupled circuits and also transistors.

To compile a book of formulae and calculations that will serve the purposes of both students and engineers is a difficult task. However, with elementary requirements of the student in mind, the engineer will be forbearing to the many references to basic principles and aspects of radio. The engineering appeal is, by and large, to engineers engaged in the transmitter side of the radio industry. It is natural that the slant of the book should be in the direction of the transmitter engineer in view of the author's well known past activity in the transmitter field. A typical section will suffice to illustrate the general contents; that on power supply, which is intended mainly for the station and installation engineer includes formulae on transmitter power, load current, power factor of load, measurement of AC power and power factor, power factor correction, efficiencies and equivalent power of engine generators, total power requirements of transmitter.

The titles of some of the sections are somewhat misleading as to their scope. For example, the one entitled "Television Principles" contains only elementary formulae relating to scanning frequencies, signal e.m.f. developed in the receiving aerial, and feeders.

This is a minor criticism of a book which will be a useful reference to engineering students and to engineers whose knowledge of mathematics has become dull with disuse.

THE DESIGN OF BAND-PASS FILTERS IN WAVEGUIDES

By S. S. FORTE, B.Sc, Ph.D.

Waveguide filters are an essential element in many applications and in particular in wide-band microwave links. The requirements are rather stringent in this instance, for the filters must have a passband of $\pm$ 12 *Mc/s while at the same time they must have a rejection of* 30 *to* 40 *dB at off-band frequencies of* $\pm$ 29 *Mc/s, this being the C.C.I.R recommended channel separation.*

The "maximally flat" type of filter is capable of achieving this performance, but necessitates a rather large number of resonant cavities (7 *to* 8).

A different type of design is therefore considered which will satisfy the specification with a minimum number of cavities.

In this article a theoretical analysis is given for the maximally flat case, starting from the low-pass, lumped element prototype, leading eventually to the classical results obtained by Mumford[1]. *This form of analysis is then applied to the "Tchebycheff equal ripple response" case, and relations are given for a complete design of such filters.*

The practical realization of the resulting network, be it a maximally flat or a Tchebycheff filter, is described.

GENERAL CONSIDERATIONS ON LOADED — Q

The loaded Q of a resonant branch in a filter is defined in terms of the insertion loss resulting when the branch is connected between a source and a receiver, each of resistance R. It can be shown, by the analysis of such a circuit (Fig. 1), that

$$\frac{P_0}{P_L} = 1 + Q_r^2 \left(\frac{f}{f_0} - \frac{f_0}{f} \right)^2$$

where f_0 is the resonant frequency of the section

f is the frequency at which the insertion loss is being measured

P_0 is the power available from the generator

P_L is the power delivered to the load

If at a frequency f_c the power delivered to the load is half the available power, then

$$\frac{P_0}{P_L} = 2$$

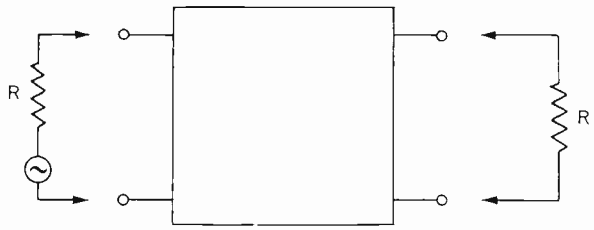

Fig. 1

and thus

$$Q_r = \frac{1}{\frac{f_c}{f_0} - \frac{f_0}{f_c}}$$

For a maximally flat filter design, the 3 dB bandwidth, and therefore f_c, is normally specified so that Q can be determined.

For another form of filter design discussed below, the 3 dB bandwidth is not specified; a certain band edge frequency f_a is specified, however, and the ratio

$$\frac{1}{\frac{f_a}{f_0} - \frac{f_0}{f_a}}$$

is used in the design of the filter, although it does not have the same meaning as the Q_r of the maximally flat filter.

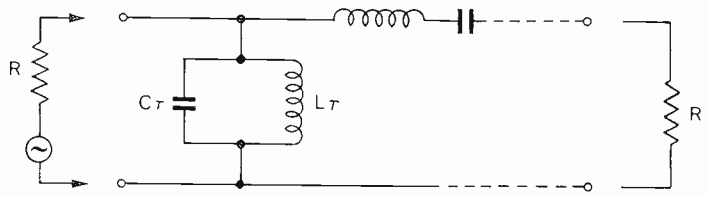

Fig. 2

A band-pass filter has the general structure shown in Fig. 2.

An alternative definition for the loaded Q of a filter section therefore follows:

For a series resonant section, the loaded Q is

$$Q_r = \frac{1}{2R}\sqrt{\frac{L_r}{C_r}} = \frac{\omega_0 L_r}{2R}$$

For a parallel resonant section, the loaded Q is

$$Q_r = \frac{R}{2}\sqrt{\frac{C_r}{L}} = \frac{\omega_0 C_r}{2} \cdot R$$

THE MAXIMALLY FLAT FILTER DESIGN

As stated in the preceding section, the loaded Q of a filter section is given by

$$Q_r = \frac{1}{\frac{f_c}{f_0} - \frac{f_0}{f_c}}$$

It follows therefore that the loaded Q of the entire filter can be given as

$$Q_T = \frac{1}{\frac{f_c}{f_0} - \frac{f_0}{f_c}}$$

where f_0 is the resonant or passband centre frequency.

f_c is the frequency at which the insertion loss through the filter is 3 dB.

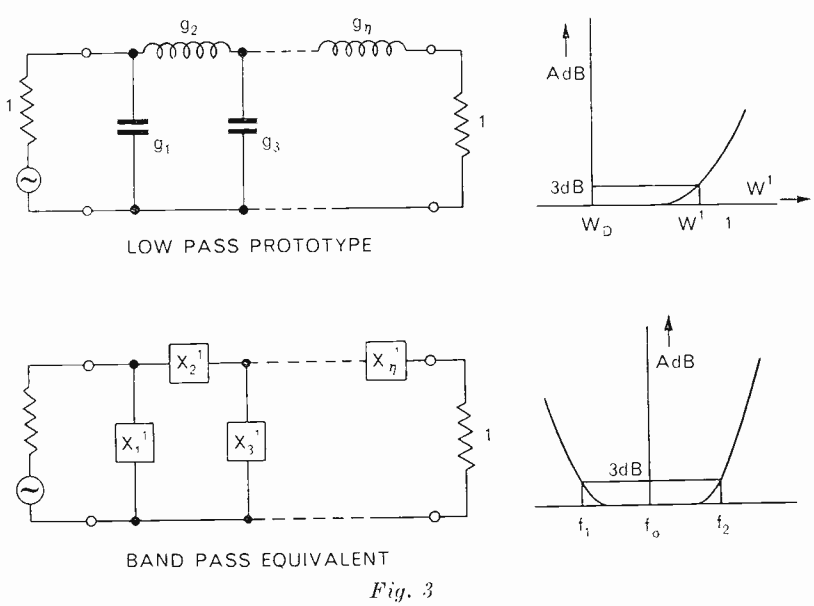

Fig. 3

Consider the low-pass lumped element prototype filter (Fig. 3). The element values for the maximally flat low-pass prototype filter normalized to $R = 1$ and $\omega_1' = 1$ at 3 dB point are

$$g_k = 2 \sin\left[\left(\frac{2k-1}{2n}\right)\pi\right]$$

where k is the number of the branch from one end of the filter

n is the total number of branches

The insertion function is

$$A = 10 \text{ Log }_{10}(1 + \omega^{2n})$$

Transformation to the band-pass equivalent is effected by the substitution

$$\frac{\omega'}{1} = \frac{\dfrac{\omega}{\omega_0} - \dfrac{\omega_0}{\omega}}{\dfrac{\omega_2}{\omega_0} - \dfrac{\omega_0}{\omega_2}} = \left(\frac{\omega}{\omega_0} - \frac{\omega_0}{\omega}\right) \cdot Q_T$$

For the low-pass prototype, the reactance of the series branch is

$$X_2 = j\omega' g_2$$

Transforming to the band-pass equivalent,

$$X_2' = j\omega \frac{g_2 Q_T}{\omega_0} + \frac{1}{j\omega \dfrac{1}{\omega_0 g_2 Q_T}}$$

X_2' therefore consists of a series resonant circuit where

$$L_2 = \frac{g_2 Q_T}{\omega_0} \qquad C_2 = \frac{1}{\omega_0 g_2 Q_T}$$

For such a series resonant section $Q_r = \dfrac{\omega_0 L_r}{2R}$

therefore $Q_2 = \dfrac{g_2 Q_T}{2R}$

Starting from the shunt branch g_1, the same result is obtained so that in general

$$Q_r = \frac{g_r Q_T}{2R}$$

Substituting for g_r

$$Q_r = Q_T \sin\left[\left(\frac{2r-1}{2n}\right)\pi\right]$$

In terms of waveguide filters, and selectivities of resonant cavities, this is the relation quoted by Mumford, between the Q's of the individual cavities and the total Q of the filter.

The insertion loss function after transformation from the low-pass prototype is

$$A = 10 \text{ Log}_{10}\left\{1 + \left[Q_T\left(\frac{f}{f_0} - \frac{f_0}{f}\right)\right]^{2n}\right\} \text{dB}$$

This again is the relation given by Mumford.

For the maximally flat design, Q_T is determined from the specified ejection at a frequency f outside the passband, and from the required WR values inside the pass band.

If $\Omega \equiv Q_T\left(\frac{f}{f_0} - \frac{f_0}{f}\right)$

he insertion loss is $A = 10 \operatorname{Log}_{10} (1 + \Omega^{2n})$

nd the SWR, S is given by the relation $\Omega^n = \frac{S-1}{2\sqrt{S}}$

By referring to curves given by Mumford, it is possible to determine

1) The value of Ω^n to give the required rejection outside the passband (i.e. Ω^n rejection).
2) The value of Ω^n to give the required SWR in the pass band (i.e. Ω^n passband).

It follows that

$$Q_T = \frac{\sqrt[n]{\Omega^n \text{ pass band}}}{\frac{f_1}{f_0} - \frac{f_0}{f_1}}$$

here f_1 is the passband edge.

$$Q_T = \frac{\sqrt[n]{\Omega^n \text{ rejection}}}{\frac{f_2}{f_0} - \frac{f_0}{f_2}}$$

here f_2 is the frequency at which the specific rejection is required.

A simultaneous solution of these two equations results in the choice of he number of cavities and the value of Q_T required to meet the specifications of the filter.

By applying the relations obtained above, the value of the Q's of the ndividual cavities is then determined.

A discussion of the determination of the physical dimensions of a avity from the value of its loaded Q is given on page 110.

HE TCHEBYCHEFF FILTER DESIGN

onsider the low-pass prototype shown in Fig. 4:

The band-pass equivalent is obtained from the low-pass prototype by he frequency transformation.

$$\frac{\omega'}{1} = \frac{\frac{\omega}{\omega_0} - \frac{\omega_0}{\omega}}{\frac{\omega_{p2}}{\omega_0} - \frac{\omega_0}{\omega_{p2}}} = \frac{\frac{f}{f_0} - \frac{f_0}{f}}{\frac{f_{p2}}{f_0} - \frac{f_0}{f_{p2}}}$$

here f_{p2} is the band edge frequency.

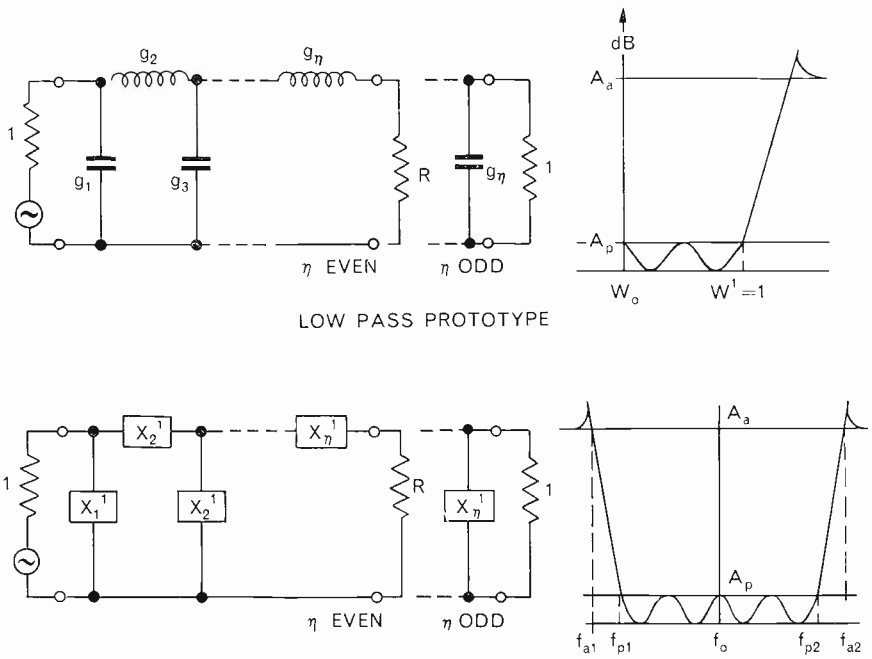

Fig. 4

The series reactance becomes

$$X_2' = j\omega \frac{g_2}{\omega_0} \frac{1}{\dfrac{f_{p2}}{f_0} - \dfrac{f_0}{f_{p2}}} + \frac{1}{j\omega \dfrac{\dfrac{f_{p2}}{f_0} - \dfrac{f_0}{f_{p2}}}{\omega_0 g_2}}$$

Let the quantity $\dfrac{1}{\dfrac{f_{p2}}{f_0} - \dfrac{f_0}{f_{p2}}} = Q_T'$

then for the series resonant arm, $X_2' = j\omega L_2 + \dfrac{1}{j\omega C_2}$

$$Q_2 = \frac{\omega_0 L_2}{2R} = \frac{g_2 Q_T'}{2R}$$

Similarly for the shunt arm.

In general, the value of the loaded Q of a resonant branch in a network between a generator of resistance R and a load resistance R becomes

$$Q_r = \frac{G_r Q_T'}{2R}$$

where Q_T' does not represent the total Q of the filter as in the maximally

at case, but is a convenient notation for the quantity

$$\frac{1}{\dfrac{f_{p2}}{f_0} - \dfrac{f_0}{f_{p2}}}$$

where G_r is the actual element value for the prototype network for a load resistance R.

The following relations hold for the element values of the low-pass prototype where the generator resistance is $R_g = 1$.

$$g_1 = \frac{2a_1}{\gamma}$$

$$g_r = \frac{4a_{r-1}\,a_r}{b_{r-1}\,g_{r-1}}$$

where $a_r = \sin\left[\left(\dfrac{2r-1}{2n}\right)\pi\right]$

$$b_r = \gamma^2 + \sin^2\frac{r\pi}{n}$$

$$\gamma = \sinh\frac{\beta}{2n}$$

$$\beta = \mathrm{Log_e}\left(\coth\frac{A_p}{17{\cdot}37}\right) \text{ where } A_p \text{ is measured in dB.}$$

Moreover, $g_n = R \times g_1$

The insertion function for the band-pass filter, after transformation from the function for the low-pass prototype becomes

$$A = 10\ \mathrm{Log_{10}}\left[1 + \left(10^{\frac{A_p}{10}} - 1\right)\cos^2\left(n\cos^{-1}\left\{\left(\frac{f}{f_0} - \frac{f_0}{f}\right)Q_T'\right\}\right)\right]\mathrm{dB}$$

$$\text{for } \left(\frac{f}{f_0} - \frac{f_0}{f}\right)Q_T' \leqslant 1$$

$$A = 10\ \mathrm{Log_{10}}\left[1 + \left(10^{\frac{A_p}{10}} - 1\right)\cosh^2\left(n\cosh^{-1}\left\{\left(\frac{f}{f_0} - \frac{f_0}{f}\right)Q_T'\right\}\right)\right]\mathrm{dB}$$

$$\text{for } \left(\frac{f}{f_0} - \frac{f_0}{f}\right)Q_T' \geqslant 1$$

The relations between the cavities differ for the cases of filters with an *even* or an *odd* number of cavities. These two cases will therefore be treated separately.

ODD NUMBER OF CAVITIES

When n is *odd*, the final element of the prototype filter is a capacitance, and the load resistance becomes

$$R = 1$$

$$G_r = g_r$$

and the cavity selectivities for the waveguide filter are determined as

$$Q_1 = \frac{a_1}{\gamma} Q_T'$$

$$Q_r = \frac{2a_{r-1}\, a_r}{b_{r-1}\, g_{r-1}} Q_T'$$

For a five-cavity filter, the prototype values become

$$g_1 = \frac{2a_1}{\gamma}$$

$$g_2 = \frac{2a_2\gamma}{b_1}$$

$$g_3 = \frac{2a_3 b_1}{b_2\gamma}$$

$$g_4 = \frac{2a_4 b_2\gamma}{b_1 b_3}$$

$$g_5 = \frac{2a_5 b_1 b_3}{b_2 b_4 \gamma}$$

where

$$a_1 = a_5 = \sin\frac{\pi}{10}$$

$$a_2 = a_4 = \sin\frac{3\pi}{10}$$

$$a_3 = \sin\frac{\pi}{2}$$

and where

$$b_1 = b_4 = \gamma^2 + \sin^2\frac{\pi}{5}$$

$$b_2 = b_3 = \gamma^2 + \sin^2\frac{2\pi}{5}$$

The cavity selectivities are then

$$Q_1 = \frac{a_1}{\gamma} Q_T'$$

$$Q_2 = \frac{a_2 \gamma}{b_1} Q_T'$$

$$Q_3 = \frac{a_3 b_1}{b_2 \gamma} Q_T'$$

$$Q_4 = \frac{a_4 b_2 \gamma}{b_1 b_3} Q_T'$$

$$Q_5 = \frac{a_5 b_1 b_3}{b_2 b_4 \gamma} Q_T'$$

Substituting for a_4, a_5, b_3, b_4 in terms of a_1, a_2, b_1, b_2 and simplifying, we get finally

$$Q_1 = Q_5 = \frac{a_1}{\gamma} Q_T'$$

$$Q_2 = Q_4 = \frac{a_2 \gamma}{b_1} Q_T'$$

$$Q_3 = \frac{a_3 b_1}{b_2 \gamma} Q_T'$$

In the above expressions a_1, a_2, a_3 are determined once the number of cavities has been fixed to five.

b_1, b_2, γ are determined by the choice of the passband ripple.

Q_T' depends upon the "off-band" frequency and the centre frequency.

As an example, for a five-cavity filter with a passband ripple, in the insertion loss characteristic, of 0·01 dB (0·83 dB ripple in the SWR characteristic), the selectivity relations are

$$Q_1 = Q_5 = 0{\cdot}336\, Q_T'$$

$$Q_2 = Q_4 = 0{\cdot}625\, Q_T'$$

$$Q_3 = 0{\cdot}740\, Q_T'$$

EVEN NUMBER OF CAVITIES

For *n even*, the load resistance is not 1 but a value dependent upon the passband ripple, namely $R = \tanh^2 \frac{\beta}{4}$.

The prototype values $g_1, g_2, g_3 \ldots\ldots g_n$, must be corrected by a factor R, so that

$$G_1 = g_1 \times R$$

$$G_2 = g_2 \times R$$

$$G_3 = g_3 \times R$$

etc., and for a four-cavity filter these values become

$$G_1 = \frac{2a_1}{\gamma} R$$

$$G_2 = \frac{2a_2\,\gamma}{b_1}$$

$$G_3 = \frac{2a_3\,b_1}{b_2\,\gamma} R$$

$$G_4 = \frac{2a_4\,b_2\gamma}{b_1\,b_3}$$

whence the cavity selectivities become

$$Q_1 = \frac{a_1}{\gamma} Q_T'$$

$$Q_2 = \frac{1}{R} \cdot \frac{a_2\,\gamma}{b_1} Q_T'$$

$$Q_3 = \frac{a_3\,b_1}{b_2\gamma} Q_T'$$

$$Q_4 = \frac{1}{R} \cdot \frac{a_4\,b_2\,\gamma}{b_1\,b_3} Q_T'$$

for a four-cavity filter $R = \frac{g_4}{g_1} = \frac{b_2\,\gamma^2}{b_1^2}$

Moreover

$$a_1 = a_4 = \sin\frac{\pi}{8}$$

$$a_2 = a_3 = \sin\frac{3\pi}{8}$$

$$b_1 = b_3 = \gamma^2 + \frac{1}{2}$$

$$b_2 = \gamma^2 + 1$$

$$b_4 = \gamma^2$$

whence $Q_2 = \frac{a_2 \gamma}{b_1} \cdot \frac{{b_1}^2}{b_2 \gamma^2} \cdot {Q_T}' = \frac{a_2 b_1}{b_2 \gamma} {Q_T}' = \frac{a_3 b_1}{b_2 \gamma} {Q_T}' = Q_3$

$$Q_4 = \frac{a_4 b_2 \gamma}{{b_1}^2} \cdot \frac{{b_1}^2}{b_2 \gamma^2} \cdot {Q_T}' = \frac{a_1}{\gamma} {Q_T}' = Q_1$$

so that finally for a four-cavity filter

$$Q_1 = Q_4 = \frac{a_1}{\gamma} {Q_T}'$$

$$Q_2 = Q_3 = \frac{a_2 b_1}{b_2 \gamma} {Q_T}'$$

SUMMARY OF RELATIONS FOR THREE, FOUR, FIVE AND SIX CAVITY FILTERS

It is seen that no general relations for the cavity selectivities hold. Specific relations can be given for filters with a specified number of cavities.

In practice three, four, five and six cavity filters would meet most requirements, so that the relations for the selectivities of these four types will be given:

Three-Cavity Filter:

$$Q_1 = Q_3 = \frac{a_1}{\gamma} {Q_T}'$$

$$Q_2 = \frac{a_2 \gamma}{b_1} {Q_T}'$$

Four-Cavity Filter:

$$Q_1 = Q_4 = \frac{a_1}{\gamma} {Q_T}'$$

$$Q_2 = Q_3 = \frac{a_3 b_1}{b_2 \gamma} {Q_T}'$$

Five-Cavity Filter:

$$Q_1 = Q_5 = \frac{a_1}{\gamma} {Q_T}'$$

$$Q_2 = Q_4 = \frac{a_2 \gamma}{b_1} {Q_T}'$$

$$Q_3 = \frac{a_3 b_1}{b_2 \gamma} {Q_T}'$$

Six-Cavity Filter:

$$Q_1 = Q_6 = \frac{a_1}{\gamma} Q_T'$$

$$Q_2 = Q_5 = \frac{a_2 b_1 b_3}{b_2^2 \gamma} Q_T'$$

$$Q_3 = Q_4 = \frac{a_3 b_1}{b_2 \gamma} Q_T'$$

COMPARISON BETWEEN MAXIMALLY FLAT AND TCHEBYCHEFF FILTERS

As an example of the difference in performance achieved by the two types of filters, a design for a filter in the 4,000 Mc/s band is considered. The minimum SWR in the passband is 0·91 (0·83 dB) at ± 12 Mc/s. The rejection at $f_0 \pm 30$ Mc/s is then calcuiated

No. of Cavities	Rejection at ± 30 Mc/s in dB	
	Maximally flat	Tchebycheff
3	6·0	8·7
4	8·5	22
5	15	35
6	23	47
7	30	

It is therefore evident that in many instances the specifications are such as to require a Tchebycheff equal ripple response, in order to achieve the large bandwidth in the passband together with the desired rejection outside the passband for a minimum number of cavities.

DESIGN OF THE FILTER

CAVITY DESIGN

Having determined the selectivity of each cavity by either of the methods of design outlined above, depending on the filter requirements, it now remains to translate these values into physical dimensions of a cavity in a waveguide.

A correction must be made to the calculated value of cavity Q to take into account the selectivities of the connecting lines. Mumford shows that a reduction of $\frac{\pi}{8}$ for each adjacent coupling length, in the case of quarter

wave coupling $\left(\text{or } \frac{3\pi}{8} \text{ in the case of three-quarter wave coupling}\right)$ is required. The design of the cavity follows from the corrected value of selectivity.

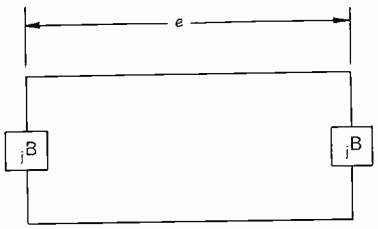

Fig. 5

The cavities consist of two identical susceptances separated by a length of waveguide (Fig. 5). The susceptances are realized by means of brass cylindrical posts centrally located in the broad face of the waveguide parallel to the electric vector.

The Marcuvitz[2] equivalent circuit for a solid inductive post in a waveguide (Fig. 6) is used throughout this design.

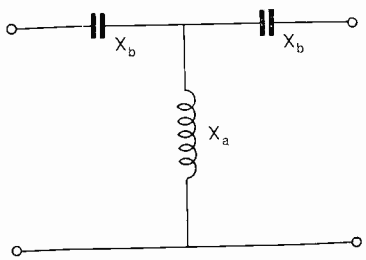

Fig. 6

The normalized reactance of the shunt inductance X_a, and the normalized reactance of the series capacitance X_b are given by the relations

$$2X_a - X_b = \frac{a}{\lambda g}\left[S_0 - \left(\frac{\pi d}{2\lambda}\right)^2 - \frac{5}{8}\left(\frac{\pi d}{2\lambda}\right)^4 - 2\left(\frac{\pi d}{2\lambda}\right)^4 \left(S_2 - 2S_0\frac{\lambda^2}{\lambda g^2}\right)^2\right]$$

$$X_b = \frac{a}{\lambda g}\left[\frac{\left(\frac{\pi d}{a}\right)^2}{1 + \frac{1}{2}\left(\frac{\pi d}{2}\right)^2\left(S_2 + \frac{3}{4}\right)}\right]$$

where a = internal broad dimension of the guide

d = post diameter

λ = free space wavelength

λ_g = waveguide wavelength

$$S_0 = \mathrm{Log_e}\frac{4a}{\pi d} - 2 + 2\sum\left[\frac{1}{n^2 - \left(\frac{2a}{\lambda}\right)^2} - \frac{1}{n}\right]$$

$$S_2 = \mathrm{Log_e}\frac{4a}{\pi d} - \frac{5}{2} + \frac{11}{3}\left(\frac{\lambda}{2a}\right)^2 - \left(\frac{\lambda}{a}\right)^2\left[\sqrt{n^2 - \left(\frac{2a}{\lambda}\right)^2} - \mathrm{n} + \frac{2}{n}\left(\frac{a}{\lambda}\right)^2\right]$$

$n = 3, 5, 7 \ldots\ldots\ldots\ldots$ to infinity

For filters in the 4,000 Mc/s band, in No. 11 waveguide ($2\frac{1}{2}$ inches by $1\frac{1}{4}$ inches) a set of solutions for these equations have been derived by Broad and Rawlinson([3]) in the form of a family of curves from which values of post diameters and cavity lengths can be directly evaluated. For filters in other frequency bands, these curves do not apply.

A set of generalized curves from the Marcuvitz equations has been computed which can be used for any frequency band, by accepting an additional parameter $\frac{\lambda}{a}$, where a is the broad dimension of the waveguide to be used ([4]).

From these results, being given the selectivity of the cavity, it is possible to determine

(1) The diameter of the post

(2) The shunt reactance X_a

(3) The series reactance X_b

The cavity length is then calculated from

$$l = \frac{\lambda_g}{2\pi}\tan^{-1}\frac{-2(X_a - X_b)}{1 + X_b(2X_a - X_b)}$$

It can be seen that by putting $X_b = 0$, this reduces to

$$l = \frac{\lambda_g}{2\pi}\tan^{-1}(-2X_a) = \frac{\lambda_g}{2\pi}\tan^{-1}\left(-\frac{2}{B}\right)$$

which is the simplified formula given by Mumford.

A correction must be made to this length to allow for the insertion of a tuning screw. Normally, a reduction in length equivalent to an increase of the centre frequency of approximately 15 Mc/s is sufficient to account for eight to nine turns of an 8 BA tuning screw.

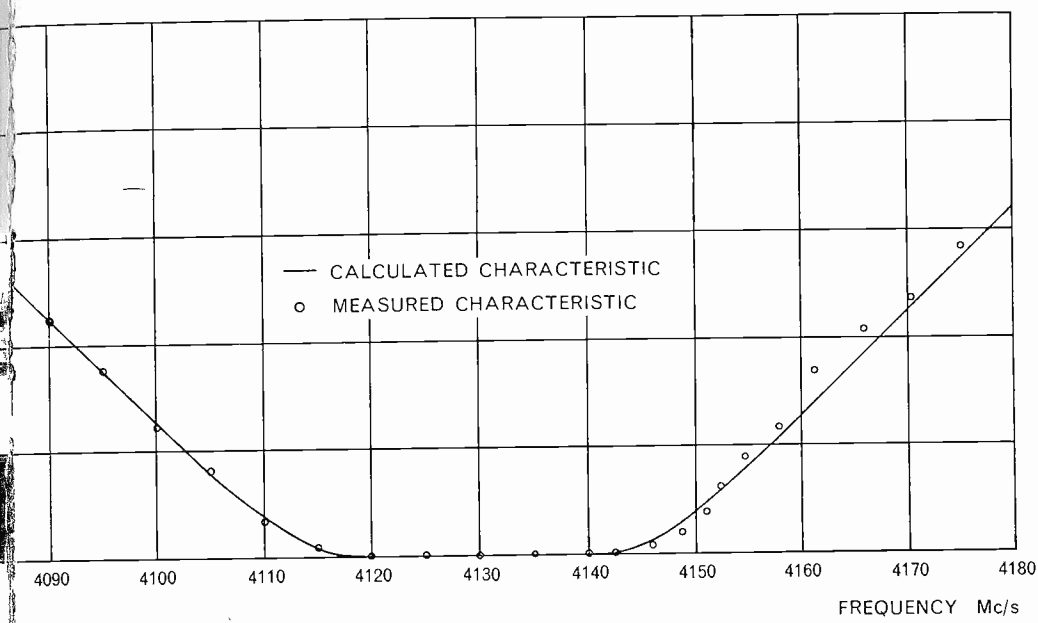

Fig. 7. Typical insertion characteristic of a maximally flat four-cavity filter

oupling Lengths

sing single-post obstacles, the spacing between individual cavities will ave to be about $\frac{\cdot 3}{4}\lambda_g$ to avoid spurious mode coupling.

A correction is required to take into account the excess phase of the avities.

The coupling length between two cavities of lengths l_1 and l_2 respectively therefore

$$l_{c12} = \frac{\lambda_g}{4} + \frac{l_1 + l_2}{2}$$

The design of the filter is thus complete.

EXPERIMENTAL RESULTS

AVITY SELECTIVITIES

ests were carried out on single cavities consisting of two brass posts eparated by a length of waveguide. Several sizes of posts were used in oth No. 11 and No. 14 waveguide. Close agreement, within less than 2% vas found between the measured values of cavity selectivities and the heoretical values calculated on the basis of the Marcuvitz equivalent ircuit, using the Huttly curves.

AXIMALLY FLAT FILTERS

Several filters of the maximally flat design were made for the prototype model of the Marconi 4,000 Mc/s radar link([5]), SX101. Good agreement between theoretically calculated responses and laboratory measured responses was observed, as illustrated in Figs. 7 and 8.

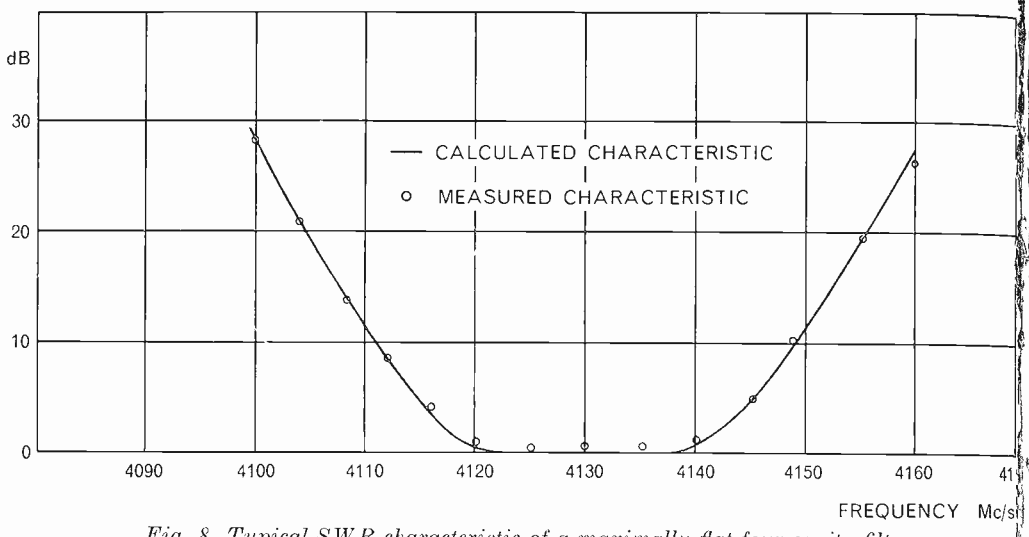

Fig. 8. Typical SWR characteristic of a maximally flat four-cavity filter

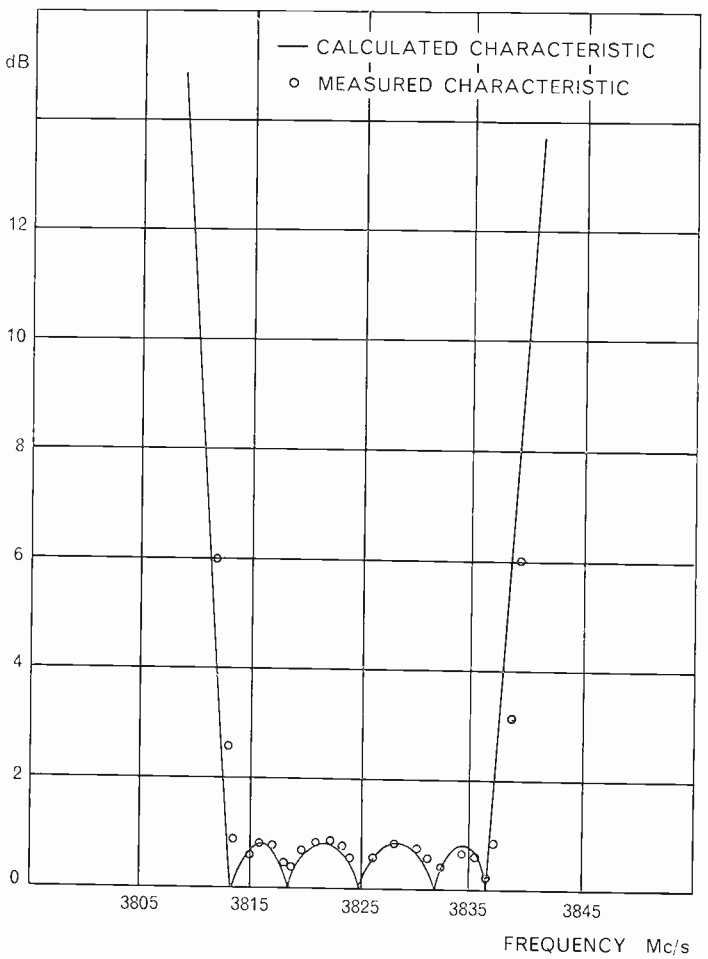

Fig. 9. Typical SWR characteristic of a Tchebycheff five-cavity filter

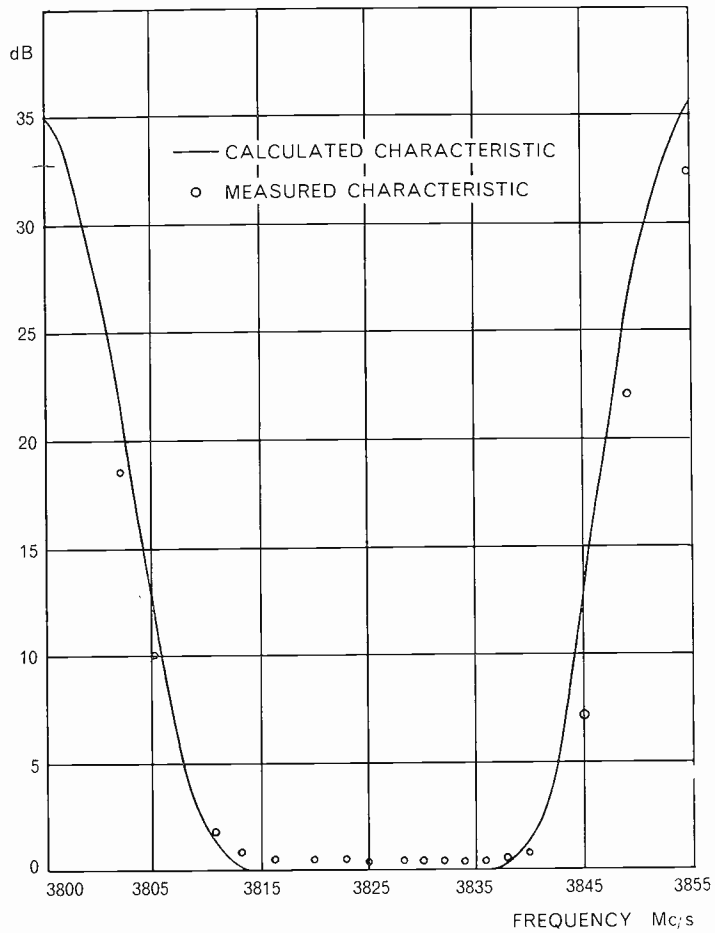

Fig. 10. Typical insertion characteristic of a Tchebycheff five-cavity filter

HEBYCHEFF FILTERS

prototype Tchebycheff-response filter has been made and tested, and, can be seen in Figs. 9 and 10, the calculated and measured responses o not differ appreciably.

ONCLUSIONS

ne design of waveguide band-pass filters of the maximally flat and Tchebycheff equal ripple" types has been discussed in detail.

A theoretical analysis is given leading to design calculations for the vity selectivities of filters of both types and to design formulae to anslate these selectivities into actual waveguide cavity dimensions.

Experimental results show good agreement with the theoretically pected characteristics.

The initial choice of filter response must be based on the passband and fband requirements. A maximally flat filter is naturally preferable for

certain applications, such as multichannel work where a very good VSW must be maintained in the passband. For other applications where certain ripple can be tolerated, the Tchebycheff type of filter will result i a wide passband together with higher rejection in the offband region f the same number of cavities.

BIBLIOGRAPHY

1 W. W. MUMFORD: Maximally Flat Filters in Waveguide. *B.S.T.J.* Vol. 27 (1948).
2 N. MARCUVITZ: *Waveguide Handbook* (M.I.T. Radiation Lab. Series, Vol. 10).
3 E. R. BROAD and W. A. RAWLINSON: Cylindrical Posts and Post-Type Cavities waveguide $2\frac{1}{2}$ inches by $1\frac{1}{4}$ inches. *P.O.E.D. Radio Report* 2278 (1953).
4 M. HUTTLY: Computation of the Equivalent Reactances and the Q-parameters f Resonant Cavities with Cylindrical Posts. *Internal Report* (1957).
5 S. S. FORTE: Waveguide Filters and Branching Networks for the Prototype Model the Marconi 4,000 Mc/s link. *Internal Report* (1957).
6 S. B. COHN: Direct Coupled Resonator Filters. *Proc. I.R.E.* (Feb. 1957).